

Disorder-induced Purcell enhancement in nanoparticle chains

Mihail Petrov*

Center of Nanophotonics and Metamaterials, ITMO University, Birjeva Line V.O. 14, 199034 Saint Petersburg, Russia

(Received 28 November 2014; revised manuscript received 26 January 2015; published 17 February 2015)

In this paper we report on a numerical study of plasmonic nanoparticle chains with long-range dipole-dipole interaction. We have shown that introduction of positional disorder gives a peak in the density of resonant states at the frequency of individual nanoparticle resonance. This peak is referred to as Dyson singularity in one-dimensional disordered structures and, according to our calculations, governs the spectral properties of local density of states. This provides disorder-induced Purcell enhancement that can find applications in random lasers and for surface-enhanced Raman-scattering spectroscopy. We stress that this effect relates not only to plasmonic nanoparticles but also to an arbitrary chain of nanoparticles or atoms with resonant polarizabilities.

DOI: [10.1103/PhysRevA.91.023821](https://doi.org/10.1103/PhysRevA.91.023821)

PACS number(s): 42.25.Dd, 78.67.Bf, 73.20.Mf

I. INTRODUCTION

Plasmonic and dielectric nanoparticle chains have been actively studied due to their subwavelength waveguiding properties in a number of papers for the last decade [1–13]. Rapidly developing self-assembly fabrication methods allow producing nanostructures with simple and cost-effective techniques [14–18]. One of the main features of self-assembly methods is the randomness and disorder in the fabricated structures. Spatial order and periodicity play key roles in the process of efficient energy transport, and introduction of disorder leads to suppressing the transmission efficiency [19–21]. However, the roles of disorder in photonics and plasmonics have been recently reconsidered. The experimental advances in random lasing [22,23] stimulated studies on light transport and photon management in disorder media [24–26]. In this paper we discuss the utilization of disorder to induce Purcell enhancement (PE) in resonant chains.

Since the early works of Mott and Anderson one-dimensional (1D) disordered structures have been attracting intensive interest from researchers. Worth noting is the monography of Lifshits *et al.* [27] almost fully dedicated to disorder in one dimension. In photonics, disordered one-dimensional photonic crystals have been studied in a number of papers [28–30]. We focus on nanoparticle chains that are quasi-one-dimensional as they are embedded in three dimensions, but the chain excitations propagate along the chain direction only. In this prospective it was shown [19,20] that introduction of disorder in nanoparticle chains stimulates scattering and increases losses. On the other hand, the randomness in plasmonic structures can be beneficial and give rise to giant fluctuations of local fields and to accumulation of energy in “hot spots” [31,32] and finds its application in surface-enhanced Raman-scattering (SERS) spectroscopy.

In this paper we report on how disorder can be utilized to control and engineer optical properties of a resonant nanoparticle chain. We demonstrate that in a one-dimensional chain the positional disorder stimulates formation of special modes that gives its contribution to density of states (DOS). Such behavior was predicted by Dyson in 1953 [33] for a chain of mechanical

oscillators with randomness. He showed that at zero energy there exists divergence in the DOS function. Such divergence was also predicted for phonon spectra of solids [34,35] and excitonic structures in disordered 1D J aggregates [36–38], and mathematically all these systems can be merged within the theory of random matrices [39,40]. Being disorder induced and, in this sense, disorder protected, the effect of divergent DOS can be implemented for local density of states (LDOS) control and spontaneous emission engineering via the Purcell effect [41–43]. This opens a route for fabrication of random lasers in one-dimensional structures and for additional SERS enhancement in disorder plasmonic chains.

The paper is structured as follows: in Sec. II we formulate our approach to the problem considering a disordered nanoparticle chain as an array of radiating plasmonic dipoles. In Sec. III the problem is treated in quasistatic (QS) and nearest-neighbor (NN) interaction limits. We show that there exists a singularity in the DOS function at the frequency of an isolated nanoparticle resonance. In Sec. III B we show that the considered simple model partially explains the basic physics lying beyond the discussed effects. In Sec. IV a more realistic approach with long-range interaction and retardation effects is proposed. We include near, intermediate, and far fields into consideration and show that Dyson peculiarity still persists in the DOS spectra. Finally, in Sec. V we discuss the Dyson peak in LDOS and demonstrate how it is influenced by ohmic losses. In Appendix A we describe the method of eigenfrequency calculation. In Appendix B the case of a non-1D (planar) nanoparticle array is considered in the example of a double line chain. The sufficient difference between the DOS spectrum and 1D chain is discussed.

II. FORMULATION OF THE PROBLEM**A. Material constants and polarizabilities**

We consider a chain of plasmonic nanoparticles as an example of coupled dipoles with Drude-like dielectric permittivity $\varepsilon(\omega) = \varepsilon_\infty - \omega_p^2 / \omega(\omega + i\gamma)$. Here ω_p is the plasma frequency of metal and γ is the damping constant related to ohmic losses. We consider spherical nanoparticles in vacuum with polarizability

$$\alpha = R^3 \frac{\varepsilon(\omega) - 1}{\varepsilon(\omega) + 2},$$

*trisha.petrov@gmail.com; Also at the Institute of Photonics, University of Eastern Finland, Yliopistokatu 7, 80100, Joensuu, Finland.

where R is the nanoparticle radius. Neglecting losses and assuming $\varepsilon_\infty = 1$ the resonant frequency of an individual nanoparticle has the form $\omega_0 = \omega_p / \sqrt{\varepsilon_\infty + 2}$. The polarizability can be written as

$$\alpha(\omega) = R^3 \frac{\omega_0^2}{\omega_0^2 - \omega^2}. \quad (1)$$

We use this form of polarizability through all the paper. We also neglect losses in the following sections except Sec. V, where we discuss the properties of the LDOS function. To account for retardation one can use the substitution [44]

$$\frac{1}{\alpha} \rightarrow \frac{1}{\alpha} - \frac{2}{3}ik^3, \quad (2)$$

where k is the wave vector. We use the quasistatic form of polarizability Eq. (1) in Sec. III only and the retarded form Eq. (2) in all others.

B. The system of equations

In order to study the effects of disorder we will consider finite chains consisting of N nanoparticles. Dipole interaction of particles splits the resonant frequency ω_0 and takes off the polarization degeneracy. For an infinite periodic chain the set of eigenfrequencies forms bands for transverse (T) and longitudinal (L) polarization [5,7,11]. We can write down the system of equations describing the dipole moments of nanoparticles:

$$\vec{d}_i = 4\pi k^2 \alpha(\omega) \sum_{j=1, j \neq i}^N \vec{G}_{ij}(\omega) \vec{d}_j, \quad i = 1, \dots, N. \quad (3)$$

Here $\vec{G}_{ij}(\omega) = \vec{G}_0(\vec{r}_i, \vec{r}_j, \omega) = \vec{G}_0(|\vec{r}_i - \vec{r}_j|, \omega)$ is the dyadic Green's function in the free space [44] taken in the following form:

$$\vec{G}_0(r, \omega) = \frac{\exp(ikr)}{4\pi r} \left\{ \left[1 + \frac{i}{kr} - \frac{1}{(kr)^2} \right] \vec{I} + \left[-1 - \frac{3i}{kr} + 3 \frac{1}{(kr)^2} \right] \frac{\vec{r} \otimes \vec{r}}{r^2} \right\}, \quad (4)$$

where \vec{I} is the unit 3×3 tensor. The terms (r, ω) , (ikr) , and (kr) correspond to near-field, intermediate-field, and far-field components, respectively.

The homogeneous problem describing the system has the form [5,45,46]

$$\mathbf{H}(\omega) \mathbf{d} = \frac{1}{\alpha(\omega)} \mathbf{d}, \quad (5)$$

where \mathbf{H} is $3N \times 3N$ block matrix, at the ij th ($1 \leq i, j \leq N$) position there is a matrix representation of the $\vec{G}(\omega)_{ij}$ tensor, and \mathbf{d} is a block vector of length $3N$ containing components of \vec{d}_i at the i th position. The homogeneous system (5) has a nontrivial solution if the condition

$$\det \left(\mathbf{H}(\omega) - \frac{1}{\alpha(\omega)} \mathbf{I} \right) = 0 \quad (6)$$

is fulfilled, where \mathbf{I} is the unity matrix. Solving this equation one can find all the resonant frequencies of the system [5]. However, for ensembles with large N this appears to be

a complicated problem. We propose using the perturbation method, and we represent $\mathbf{H}(\omega) = \mathbf{H}(\omega_0) + \delta \mathbf{H}(\omega_0)$ based on weak dependence of matrix \mathbf{H} on ω . In this case the inverse polarizability plays the role of the $\mathbf{H}(\omega_0)$ matrix eigen-number [45,47]. The eigenfrequencies can be found within the first-order precision: $\omega_n = \omega_n^0 + \omega_n^1$. More detailed description of this approach is described in Appendix A.

C. Introduction of disorder

In this paper we consider a plasmonic chain with randomly varying nanoparticle positions that is also referred to as nondiagonal disorder. Each nanoparticle can be randomly shifted around its position in the regular chain. We limit the consideration with $x-y$ plane perturbation only, keeping the chain planar (see Fig. 1). Such geometry is the most prospective from the point of possible technological realization: nanoparticle ensembles are commonly fabricated on the top of planar substrates [16,17,48]. Each nanoparticle center can be varied for a random value dx or dy . We use uniform distribution of the i th nanoparticle shift $dx_i, (dy_i)$ in the range $-\Delta_{x(y)} \leq dx(dy)_i \leq \Delta_{x(y)}$. We introduce the relative parameter of disorder $\delta_{x(y)} = \Delta_{x(y)}/a_0$, which is limited with its maximal value $\delta_{\max}(a_0)$ to restrain touching or overlapping of nanoparticles: for instance, the value of $\delta_x^{\max} \approx 0.18$ for $a_0 = 3R$.

We define two types of disorder as shown in Fig. 1: (a) $\Delta_x \neq 0, \Delta_y = 0$ longitudinal disorder (L disorder) and (b) $\Delta_x = 0, \Delta_y \neq 0$ transverse disorder (T disorder). We need to stress that L disorder keeps splitting of T and L polarizations, while T disorder mixes T and L polarizations. We also will discuss the case of planar TL disorder that is superposition of both types of disorder. We will pay much attention to L disordered chains as they have a simpler description but possess all the key properties of the considered systems.

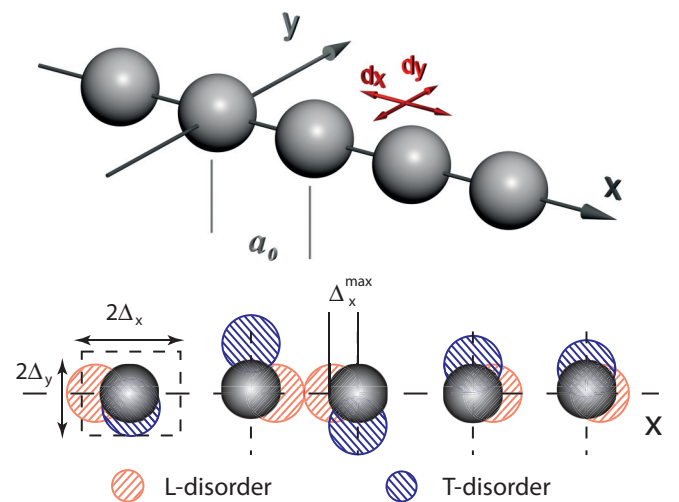


FIG. 1. (Color online) Top: Regular nanoparticle chain with fixed distance a_0 between nanoparticles. Bottom: The types of the spatial disorder: longitudinal (L) disorder relates to random position shift in the x direction; transverse (T) disorder relates to random position shift in the y direction. Δ_x^{\max} is the maximal range of a shift that provides a nonoverlapping condition.

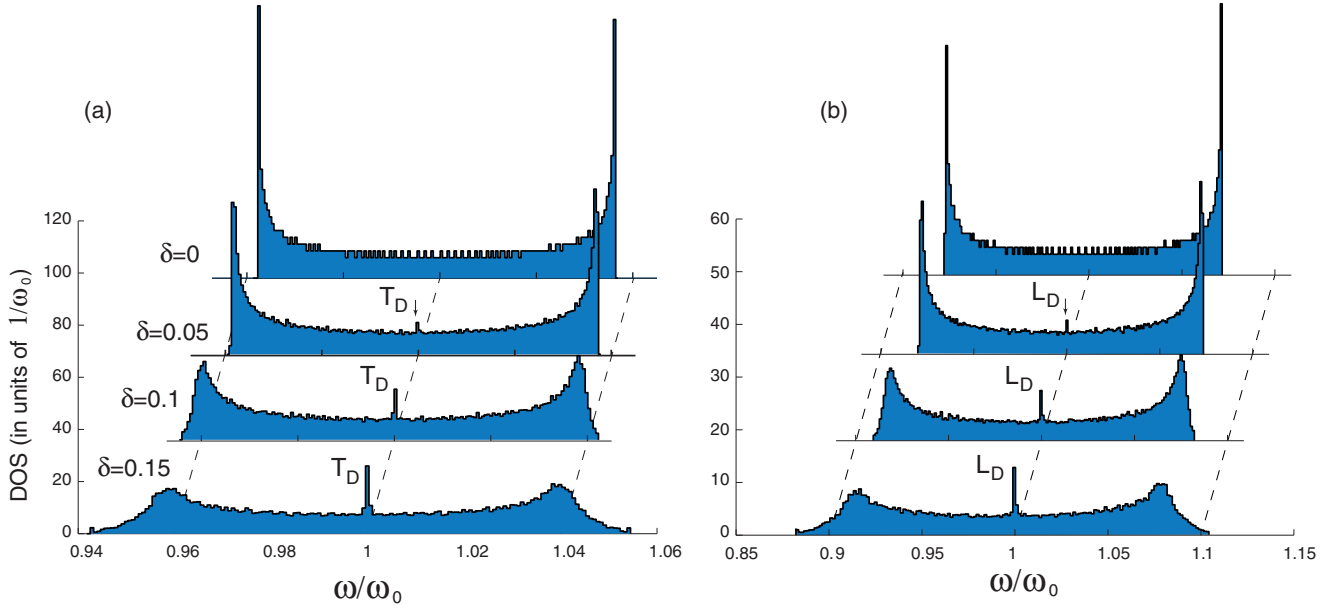


FIG. 2. (Color online) DOS in the QS limit with amplitude of L disorder. (a) T polarized modes. (b) L polarized modes. $N = 800$. The results are calculated for $a_0 = 3R$ and $N = 800$ and averaged over 50 realizations.

III. SIMPLE MODEL: QUASISTATIC AND NEAREST-NEIGHBOR INTERACTION LIMITS

We start with the consideration of nanoparticle size and interparticle distance, which is small compared with the wavelength (QS limit). The matrix \mathbf{H} depends on frequency through the term $\omega r/c$ that goes to zero in the QS limit. The matrix \mathbf{H} becomes frequency independent and, thus, real symmetric. We come to an exact eigenvalue problem with inverse polarizabilities as eigenvalues λ_k . The eigenfrequency for each eigenvalue λ_k can be found from the relation $1/\alpha(\omega_k) = \lambda_k$:

$$\mathbf{H}(0)\mathbf{d} = \lambda_k \mathbf{d} = \frac{1}{\alpha_k} \mathbf{d}.$$

In the simplest case of NN interaction the matrix \mathbf{H} has the form

$$\begin{aligned} \mathbf{H}_{i,i} &= 0, \\ \mathbf{H}_{i+1,i} = \mathbf{H}_{i,i+1} &= \frac{-1(2)}{a_{i,i+1}^3} \quad \text{for T(L) polarization} \end{aligned} \quad (7)$$

A. Regular chain

For a regular chain the distance $a_{i,i+1}$ between the particles is constant $a_{i,i+1} = a_0$ and the dispersion relation $\omega(q)$ has the form [5]

$$\begin{aligned} \omega_{T(L)}^2(q) &= \omega_0^2 [1 + g_{T(L)} \cos(qa)], \\ g_T &= 2 \frac{R^3}{a_0^3}, \quad g_L = -4 \frac{R^3}{a_0^3}, \end{aligned}$$

where q is a quasivector.

The DOS function then can be described by a simple formula that exhibits van Hove singularities at the band

edges:

$$\text{DOS}_{T(L)}(\omega) = \frac{2\omega}{\sqrt{\omega_0^4 g_{T(L)}^2 - (\omega^2 - \omega_0^2)^2}}.$$

The DOS function for a regular chain is shown in Figs. 2(a) and 2(b) at the top $\delta = 0$.

B. Longitudinal (L) disordered chain

In the case of a L disordered chain, $a_{i,i+1} = a_0 + \Delta_{i+1} - \Delta_i$ is a random number with mean value equal to a_0 and Δ_i are the nanoparticle shifts in the x direction and are given by uniform probability distribution. Thus, the system is described with a two-diagonal symmetric matrix filled with random numbers. Such a matrix was considered in the classical paper by Dyson [33]. One of the results demonstrated in this paper was a singularity of DOS at the zero eigenvalues in the limit $N \rightarrow \infty$ for nondiagonal disorder that is the case of our study. In terms of polarizability the condition of $\lambda = 0$ is satisfied at the frequency $\omega_D = \omega_0$ at which inverse polarizability has root $1/\alpha(\omega) = 1/R^3(1 - \omega^2/\omega_0^2)$. In Fig. 2 the DOS of a nanoparticle chain is presented in the QS limit and NN interaction for different values of disorder parameter δ_x . Similar behaviors were already obtained in [36–38] for excitons in one-dimensional disorder structures. The Frenkel Hamiltonian in the tight-binding limit considered in these papers has the form of Eq. (7).

The QS nearest-neighbor interaction limit gives the logarithmic divergence of the DOS function in the vicinity of the zero eigenvalue [33]. However, since the classical Dyson paper there are various discussions on the nature of the divergent states. In [49] it was shown that the states are extended and, thus, delocalized. The later studies by [37] dispute this claim. Our calculations of participation ratio also demonstrate that the localization length is finite, however [38] reports that this may be due to the finite-size effect. The appearance of this

singularity can be understood within the perturbation theory. Kozlov *et al.* [37] showed that in the QS limit introducing disorder as perturbation gives a zero shift of energy levels in the middle of the band that results in increasing of DOS.

Since the early works of Dyson and Wigner active development of the theory of random matrices has started, and sparse random matrices play an important role among them. In several papers [35,50,51] it has been shown that the singularity of DOS for the zero eigenvalue is tightly related to sparsity of random matrices. The constructed matrix (7) is just the case of a sparse random matrix. The random matrix theory predicts that this effect can be observed in the vicinity of the zero eigenvalue in a wide class of random matrices. In our terms, zero value eigenvalues correspond to resonance in polarizability. Consequently, divergent DOS behavior will be observed in a quite general class of interacting resonant oscillators, and the plasmonic particle chain is just an example.

IV. RETARDATION AND LONG-RANGE INTERACTION

The previous studies by [36,37] considered long-range dipole-dipole interaction in 1D disordered systems only in the QS regime; i.e., the interaction was governed by near fields that decrease as $\sim 1/r^3$. The long-range radiation effects play important role in plasmonics. We considered a fully retarded model with intermediate ($\sim 1/r^2$) and far ($\sim 1/r$) fields that are the major interaction terms at long distances. We demonstrate that despite stronger long-range coupling one still can observe the peculiarity at the band center.

To include the retardation effects we consider frequency dependent matrix $\mathbf{H}(\omega)$ and use substitution (2) to account for dipole emission that introduces losses in the system. We neglect ohmic losses $\gamma = 0$ at this stage, but will add them in Sec. V of the manuscript. To find the eigenfrequency of the system (5) we apply the approximate method described in Appendix A. The main parameter that defines the dependence of the \mathbf{H} matrix on frequency is $\kappa = \omega_0 R/c$. Indeed, the eigenfrequencies will lie around ω_0 and parameter κ shows the retardation strength, i.e., typical phase shift at the scales of nanoparticle radius. In this paper we are limited with small values of κ as the approximate method of calculation based on perturbation theory diverges for large κ ; thus, for all the calculations below we take $\kappa = 0.15$.

A. Regular chain

To understand the influence of disorder accounting for retardation we again start with the regular chain. The periodical nanoparticle chains accounting for retardation and losses have been extensively studied during the last decade [1–13] because of their waveguiding properties and application in plasmonics. The full and exhaustive review on this topic can be found elsewhere [52]. Here we will briefly discuss the main results related to our study. The simple QS picture with nearest-neighbor interaction does not properly describe propagation of excitation in the plasmonic chain. Despite this, even in the NN limit it was shown [1,4,5,8] that the eigenfrequencies of chain modes are complex and, thus, leaking. In the works of Weber and Ford [5] and Citrin [8] it was shown that accounting for retardation and long-range interaction dramatically changes the

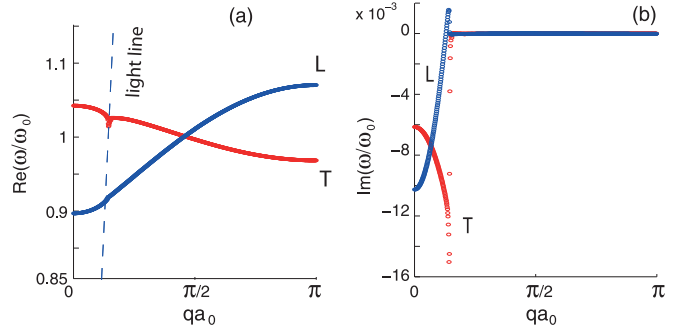


FIG. 3. (Color online) (a) Dispersion relation of a regular nanoparticle chain with retardation for T and L modes. The dispersion of light in free space (light line) is also shown. (b) Dependence of imaginary parts of eigenfrequencies on a quasivector for T and L modes. The results are calculated for $a_0 = 3R$, $\gamma = 0$, $\kappa = 0.15$, and $N = 400$.

dispersion relation and waveguiding properties of plasmonic chains. We have computed the eigenmodes of a regular chain consisting of $N = 400$ nanoparticles with our method, and the real and imaginary parts of eigenfrequencies are shown in Figs. 3(a) and 3(b) for T and L modes. The dispersion relation depicted in Fig. 3(a) was obtained by sorting the eigenmodes

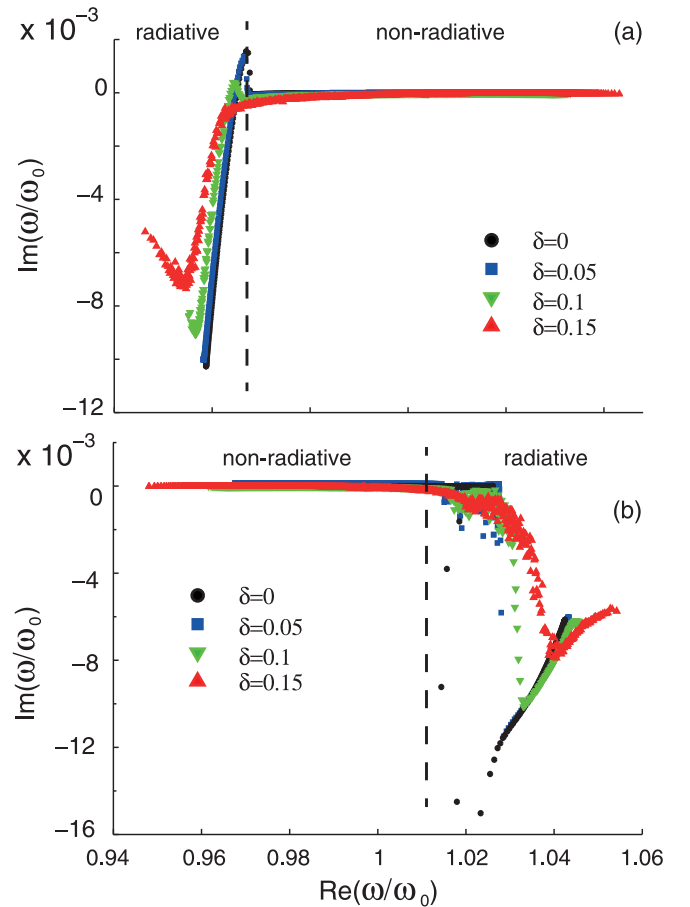


FIG. 4. (Color online) The imaginary parts of eigenfrequencies for (a) L polarization and (b) T polarization for different magnitudes of L disorder. The parameters of calculation are taken the same as in Fig. 3. Results are obtained after averaging over 50 realizations.

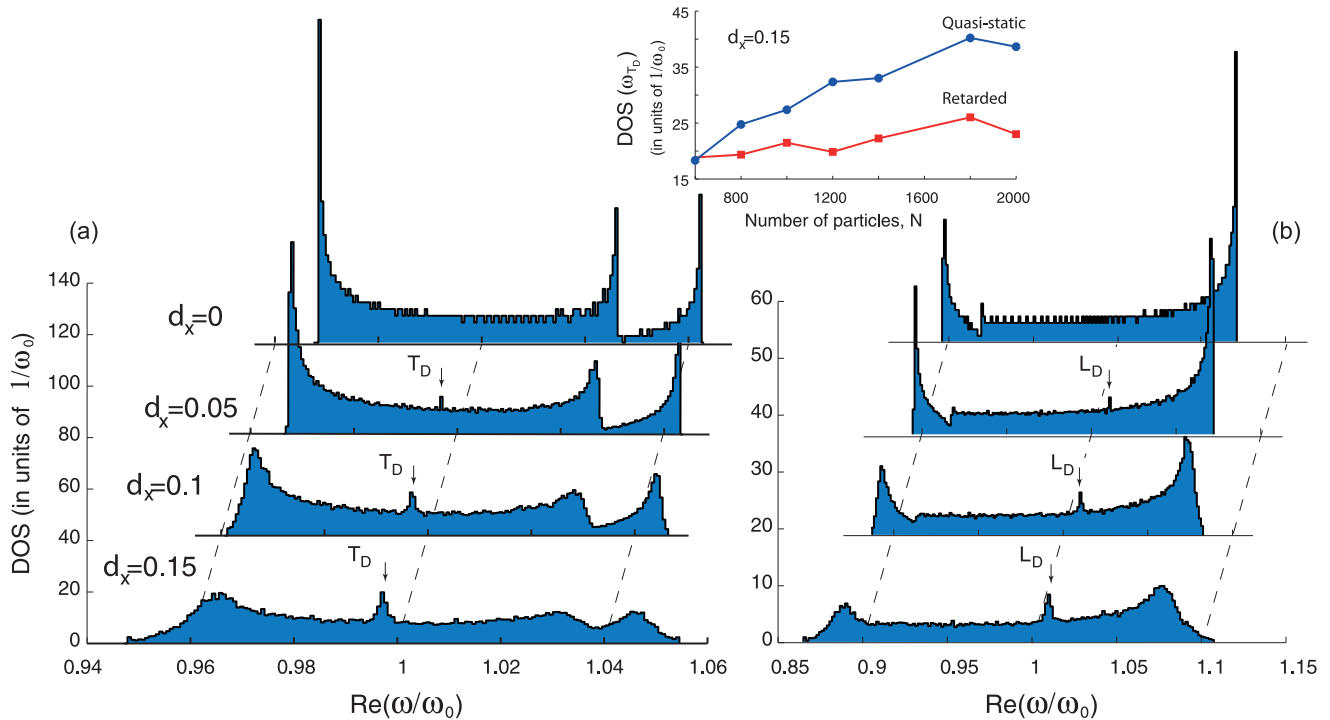


FIG. 5. (Color online) DOS for a L disordered chain with retardation for T polarized modes (a) and L polarized modes (b). The results are calculated for $a_0 = 3R$, $\kappa = 0.15$, $\gamma = 0$, and $N = 800$ and averaged over 50 realizations. Inset: DOS calculated at the frequency ω_{T_D} corresponding to the T_D peak in the quasistatic limit (see Fig. 2) (circles) and with retardation and long-range interaction (squares) depending on chain length N at fixed magnitude of disorder $\delta_x = 0.15$.

in the descending order of node numbers in the eigenvector. The Bloch vector corresponds to the number of zeros as

$$q = \frac{\pi(n+1)}{Na_0}.$$

These results are in good agreement with the result obtained previously [5,8]. According to them the T modes lying above the light line are well coupled to light and are highly radiative (super-radiative), that is confirmed by the large negative value of $\text{Im}(\omega_i)$. On the other hand, the modes below the light line are nonradiative (waveguiding regime) and are almost decoupled with light; however, the imaginary part is also nonzero. The strong hybridization of waveguiding modes with light is seen in the vicinity of the light line crossing with the dispersion curve. The calculation method shows discrepancy for L modes close to $ka_0 \sim 0.2$ where the imaginary part becomes positive.

B. Longitudinal (L) disordered chain

To demonstrate how disorder affects the eigenspectrum we plotted imaginary parts of eigenfrequencies in Fig. 4 for T modes (a) and for L modes (b). We see that the disordered structures inherit the properties of ordered systems for both T and L modes and we again can divide the spectral region into highly radiating and nonradiating regions. Destruction of periodicity increases losses in the nonradiative region due to additional scattering of Bloch waves on defects, but in the radiating region losses are decreased because disorder suppresses the super-radiative regime.

To describe the properties of disordered structures we again introduce DOS similar to the QS case. However, in the case of

retardation the eigenfrequencies are complex, and we will plot the DOS depending on the real part of eigenfrequency $\text{Re}(\omega)$ (see Fig. 5).

The DOS function for a regular chain has complicated structure due to the strong hybridization of chain modes with light. With the increase of disorder the DOS function becomes more and more homogeneous. But despite the long-range interaction and retardation one can see the divergence of the DOS function near the frequency ω_0 similarly to the case of QS and NN limits. However, the DOS peak is now shifted for T and L modes compared with the case shown in Fig. 2 due to long-range interaction effects. The shift of the peak corresponds to the shift of band central frequency [37] and this shift has opposite sign for T and L modes. The DOS peak intensity increases with the increase of chain length N (see Fig. 5 inset) both in the QS and retarded case, which reflects its divergent character.

C. Planar (TL) disorder

Till now we have considered only L disorder that conserves splitting of modes into T and L polarizations. Introduction of TL disorder partially mixes mode polarization. The polarization of eigenmodes lying in the x - y plane will be mixed, and the z component of the vector will be still independent and behave similarly to y polarized modes in the case of L disorder. Thus, we will not discuss z polarized modes in this section. To emphasize, we will refer to $\text{DOS}_{||}$, meaning the density of resonant states with the polarization vector lying in the x - y plane. The influence of TL disorder on DOS is depicted in Fig. 6. One can see that introduction of weak

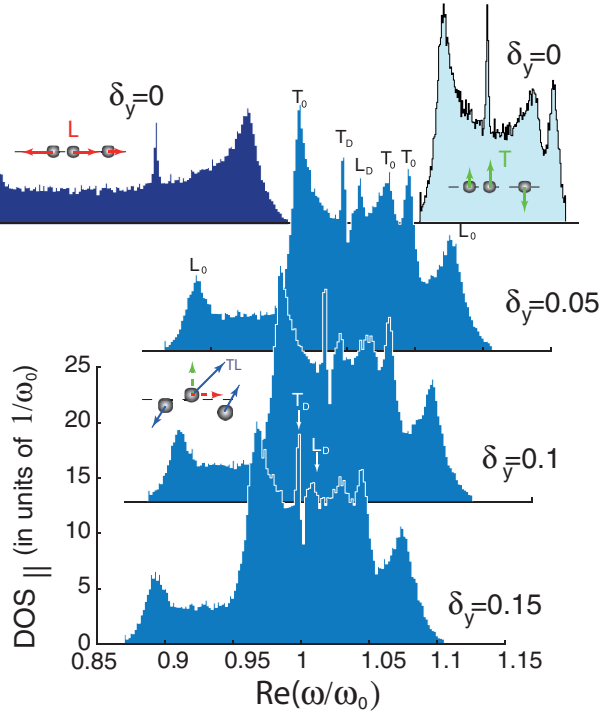


FIG. 6. (Color online) DOS function for a TL disordered chain with $\delta_x = 0.15$ and different values of δ_y . The DOS functions of T and L polarized states for a purely L disordered ($\delta_y = 0$) chain are shown separately at the top of the figure. Inset: Each dipole moment in the TL disordered mode has x and y components. For weak disorder one can divide modes into mainly T and L polarized. The peaks related to DOS of the ordered chain are denoted as T_0 and L_0 along with Dyson peaks T_D and L_D . The parameters of calculations are the same as in Fig. 5.

disorder $\delta_y = 0.05$ mixes the polarization insignificantly and the DOS function is roughly the sum of T (light colored) and L polarization (dark colored) DOS functions in a purely L disordered chain. We mark the peaks originating from the ordered T and L polarizations as T_0 and L_0 , respectively. The Dyson peaks are marked as T_D and L_D . One can see that the increase of T disorder affects the L_D peak mainly and for $\delta_y = 0.15$ the L_D is almost smeared out. The T_D peak on the other hand does not change significantly. Here we can conclude that the transversal Dyson mode (T_D) is stable with respect to transversal disorder in contrast with the longitudinal mode.

In Appendix B we have also considered the special case of a double line chain with TL disorder to demonstrate that the features of Dyson singularity originate from a 1D character of interaction. Considering two parallel chains of nanoparticles dramatically changes the DOS function, and the fine structure around ω_0 disappears.

V. LOCAL DOS AND PURCELL ENHANCEMENT

We have demonstrated that the disorder in a nanoparticle chain leads to peculiarity in the DOS function near the band center, which relates to Dyson singularity of a 1D disordered system. In nanophotonics the role of the LDOS function is of even more importance. The LDOS is connected to DOS via

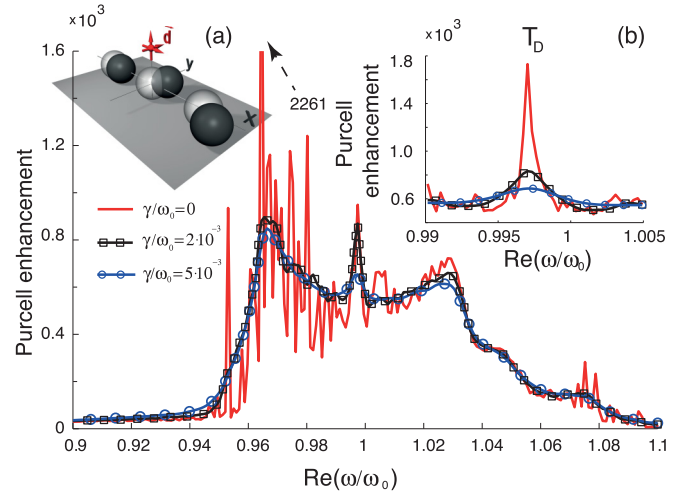


FIG. 7. (Color online) Spectrum of the Purcell enhancement factor calculated at the point $(0,0,2R)$ and plotted for different values of losses in metal. Radiation losses are also accounted. Inset: (a) The point of Purcell enhancement calculation and (b) the zoomed Purcell enhancement curve around Dyson singularity. The number of particles in the chain $N = 101$. The parameters of calculation are $\delta_x = 0.15$, $\delta_y = 0.15$, and $\kappa = 0.15$. The $\gamma = 0$ curve was obtained after averaging over 2000 realizations, and the other curves were averaged over 500 realizations. Note that in the limit $z \approx R$ the dipole model loses its accuracy.

simple relation $D(\omega) = \int \rho(\vec{r}, \omega) d^3r$; thus, one can expect that LDOS properties possess similar spectral features as DOS.

To obtain the LDOS function we have computed the dyadic Green's function $\vec{G}_{\text{tot}}(\vec{r}, \vec{r}, \omega)$ of the whole system. It can be decomposed into

$$\vec{G}_{\text{tot}}(\vec{r}, \vec{r}, \omega) = \vec{G}_0(\vec{r}, \vec{r}, \omega) + \vec{G}_{\text{sc}}(\vec{r}, \vec{r}, \omega),$$

where $\vec{G}_0(\vec{r}, \vec{r}, \omega)$ is the Green's function of the free space and $\vec{G}_{\text{sc}}(\vec{r}, \vec{r}, \omega)$ is the Green's function related to the fields scattered by the nanoparticle chain. To compute \vec{G}_{sc} we apply the following procedure: we place a dipole source at the coordinate \vec{r} [it corresponds to $(0,0,2R)$ in the Fig. 7 inset] oriented along the x , y , or z axis. Then, we compute the dipole moments of the nanoparticle chain via system (8) with dipole source field $\vec{E}_d(\vec{r})$ as an inhomogeneity in the right-hand side:

$$\vec{d}_i = \alpha(\omega) \left(\vec{E}_d(\mathbf{r}_i) + 4\pi k^2 \sum_{j=1, j \neq i}^N \vec{G}_{ij}(\omega) \vec{d}_j \right),$$

$$i = 1, \dots, N. \quad (8)$$

Calculating the electric field generated by the nanoparticles at the point of the dipole source \vec{r} we can reconstruct the xx , yy , and zz elements of \vec{G}_{sc} for x , y , and z orientation of the dipole source. Only diagonal elements of dyad \vec{G}_{sc} are required as LDOS, averaged over the dipole source orientation, can be found through the expression

$$\rho(\vec{r}, \omega) = \frac{2\omega}{\pi^2 c^2} \text{Im}[\text{Tr} \vec{G}_{\text{tot}}(\vec{r}, \vec{r}, \omega)].$$

We normalize LDOS over $\rho_0 = \omega^2/\pi^2c^3$, that is LDOS in vacuum, that gives us the Purcell enhancement (PE) factor [41]. The calculated LDOS is depicted in Fig. 7 for the TL disordered chain. The spectrum lines are plotted for different values of losses in metal. For $\gamma = 0$ only scattering losses are accounted for. Low losses lead to strong fluctuations of the PE due to very narrow resonances. The fluctuations are particularly strong for the frequency range below ω_0 that corresponds to the nonradiative regime of T modes for the periodic chain where radiative losses are small [see Fig. 3(a)]. Adding ohmic losses we significantly suppress the fluctuations and achieve a smooth LDOS line already for several hundreds of iterations. One can see that the spectrum of PE replicates the DOS spectrum of T modes [see Fig. 5(b)] with a clear Dyson peak. It is relatively weak as the length of the chain was taken as $N = 101$ to reduce computation time (the DOS function presented in Fig. 5 was computed for $N = 800$). Absence of the L_D peak relates to weak coupling of the dipole source with L modes. Indeed, coupling to L modes occurs only via near fields only for a dipole polarized in the x direction. The coupling via far field is suppressed as there are no x components of the electric field.

The spatial distribution of PE depending on dipole source position is plotted in Fig. 8 for $z > R$ at the frequency corresponding to T_D . Recalling that LDOS should be periodic in the x direction, we plot PE distribution over one unit cell only. The calculated PE is symmetric in the unit cell in the $x-y$ plane, respective to nanoparticle position in the regular chain. Thus, we plot only half of the unit-cell cross section in $x-z$ and $y-z$ planes as shown in the Fig. 8 inset. One can see that the PE distribution rapidly decreases away from the chain. We need to mention that the dipole model should not

be valid close to the nanoparticle surface around $z \lesssim R$ and $x \approx 0, y \approx 0$.

We again would like to stress that the calculated LDOS corresponds to the long-range-interacted and retarded system. The presence of peculiarity close to nanoparticle resonance ω_0 is related to the existence of resonant behavior of polarizability (existence of a root in the inverse polarizability $1/\alpha$). Thus, we predict the similar LDOS properties for a general class of a resonantly interacting oscillatory chain of different nature.

VI. CONCLUSION

We have studied a resonant nanoparticle chain with positional (nondiagonal) disorder. We have shown that disorder induces the divergence in the DOS function in the vicinity of individual nanoparticle resonance that is associated with Dyson singularity. This divergence is stronger in the quasistatic nearest-neighbor interaction limit, but also was found in a long-range interacting system with retardation effects. Such DOS structure is an internal feature of one-dimensional systems and cannot be observed in two- and three-dimensional arrays. We have shown that positional disorder affects T and L modes differently, that is related to the character of dipole-dipole coupling. The LDOS function inherits the structure of DOS and has a peak in the vicinity of an individual nanoparticle resonance. This result may be applied for the observation of Purcell enhancement and for spontaneous emission rate engineering in an interacting oscillatory chain with resonant polarizabilities. We believe that this effect can be applied for random lasing in one-dimensional structures and for additional enhancement of a SERS signal in the vicinity of disordered chains.

ACKNOWLEDGMENTS

This work was financially supported by Government of Russian Federation, Grant No. 074-U01, and by Academy of Finland, Grant No. 277141. The author would like to thank Yuri Kivshar for useful comments on the manuscript; fruitful scientific discussions with Pavel Belov, Andrey Bogdanov, and Ivan Iorsh have made this publication possible.

APPENDIX A: CALCULATION METHOD

To solve the system (5) we imply weak dependence of the matrix \mathbf{H} on frequency ω and decompose it into a series around the frequency $\omega = \omega_0$:

$$\begin{aligned} \mathbf{H}(\omega) &= \mathbf{H}(\omega_0) + \delta\mathbf{H}(\omega_0) \cdot (\omega - \omega_0) + \dots \\ &= \mathbf{H}_0 + \delta\mathbf{H}_0 \cdot (\omega - \omega_0) + \dots \end{aligned} \quad (\text{A1})$$

The matrix \mathbf{H}_0 is matrix $\mathbf{H}(\omega)$ calculated at the frequency $\omega = \omega_0$. The zeroth-order eigenvalues can be computed from the system

$$\mathbf{H}_0 \mathbf{d} = \lambda^{(0)} \mathbf{d}. \quad (\text{A2})$$

The inverse polarizability is a zeroth-order eigenvalue and the set of eigenfrequencies is computed from relation $1/\alpha(\omega_i^{(0)}) = \lambda_i^{(0)}$, where i is the number of eigenvalue and index (0) denotes zeroth-order approximation. Then we assume that

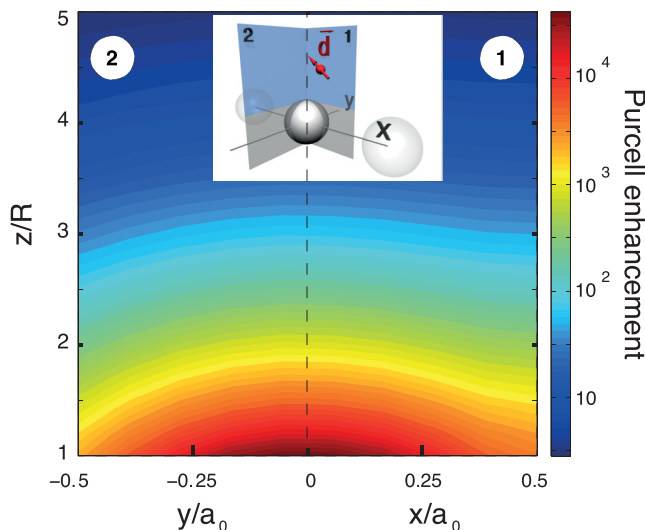


FIG. 8. (Color online) LDOS enhancement distribution for a TL disordered chain at the frequency of Dyson singularity pointed to by the arrow in Fig. 8. Due to the symmetry of the problem, LDOS is plotted only in a half of the unit cell as shown in the inset (planes 1 and 2) for $z \geq R$. The number of particles in the chain $N = 101$. The parameters of calculation are $\delta_x = 0.15$, $\delta_y = 0.15$, $\kappa = 0.15$, and $\gamma/\omega_0 = 2 \times 10^{-3}$. The result was obtained after averaging over 500 realizations.

$\lambda_i \approx \lambda_i^{(0)} + \lambda_i^{(1)}$ and the first-order correction $\lambda_i^{(1)}$ is computed with the perturbation method:

$$\lambda_i^{(1)} = \langle \bar{\mathbf{d}}_i^0 | \delta \mathbf{H}_0 \cdot (\omega_i - \omega_0) | \mathbf{d}_i^0 \rangle.$$

Here we use quasiscalar product $\langle \bar{\mathbf{a}} | \mathbf{b} \rangle = \sum_i a_i b_i$ as matrix \mathbf{H} is complex symmetric but non-Hermitian [47].

Such an approach is valid as long as the perturbation term $\delta \mathbf{H}_0 \cdot (\omega - \omega_0)$ is small. The matrix $\mathbf{H}(\omega)$ depends on frequency in the form of kr , and $\delta \mathbf{H}(\omega) \sim R/c\mathbf{H}(\omega)$. The perturbation term is smaller by a factor of $\omega_0 R/c(\omega_i - \omega_0)/\omega_0 = \kappa \delta \omega_i$ than \mathbf{H}_0 . From the QS limit the estimation of bandwidth gives $\delta \omega \sim (R/a_0)^3$. Thus, the perturbation method should be valid if $\kappa(R/a_0)^3 \ll 1$. For the parameters of calculation used in this study $\kappa = 0.15$ and $a_0 = 3R$ this condition is fulfilled.

APPENDIX B: TWO LINE CHAIN

The dimensionality of the structure plays an important role for the observed DOS peak. To demonstrate this, we have calculated the in-plane DOS function (see Sec. IV C) for a double line chain of nanoparticles separated with distance a_0 from each other in the y direction. The calculated DOS for in-plane modes in the QS limit is shown in Fig. 9. One can see that the fine structure of the DOS is totally smeared out for the double line chain. Introduction of retardation only enhances this effect. Thus, despite the fact that the system

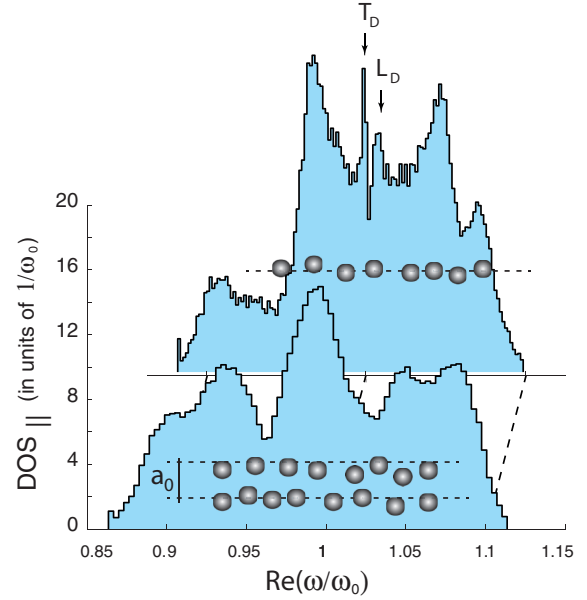


FIG. 9. (Color online) Comparison of $\text{DOS}_{||}$ functions for a double nanoparticle chain with $N = 400$ and nanoparticle array $2 \times N$ calculated in the QS limit. The disorder parameters are $\delta_x = 0.15$ and $\delta_y = 0.15$. The separation distance between the chain lines is a_0 .

is embedded in three dimensions the quasi-one-dimensional feature of the nanoparticle chain is crucial for the observed Dyson peak.

-
- [1] M. Quinten, A. Leitner, J. R. Krenn, and F. R. Aussenegg, *Opt. Lett.* **23**, 1331 (1998).
- [2] M. L. Brongersma, J. W. Hartman, and H. A. Atwater, *Phys. Rev. B* **62**, R16356 (2000).
- [3] B. S. A. Maier, M. L. Brongersma, P. G. Kik, S. Meltzer, A. A. G. Requicha, and H. A. Atwater, *Adv. Mater.* **13**, 1501 (2001).
- [4] S. Y. Park and D. Stroud, *Phys. Rev. B* **69**, 125418 (2004).
- [5] W. H. Weber and G. W. Ford, *Phys. Rev. B* **70**, 125429 (2004).
- [6] Q.-H. Wei, K.-H. Su, S. Durant, and X. Zhang, *Nano Lett.* **4**, 1067 (2004).
- [7] C. R. Simovski, A. J. Viitanen, and S. A. Tretyakov, *Phys. Rev. E* **72**, 066606 (2005).
- [8] D. S. Citrin, *Nano Lett.* **4**, 1561 (2004).
- [9] D. Citrin, *Nano Lett.* **5**, 985 (2005).
- [10] A. Alù, P. A. Belov, and N. Engheta, *New J. Phys.* **13**, 033026 (2011).
- [11] S. Campione, S. Steshenko, and F. Capolino, *Opt. Exp.* **19**, 18345 (2011).
- [12] R. Noskov, P. Belov, and Y. Kivshar, *Sci. Rep.* **2**, 873 (2012).
- [13] R. S. Savelev, D. S. Filonov, P. V. Kapitanova, A. E. Krasnok, A. E. Miroshnichenko, P. A. Belov, and Y. S. Kivshar, *Appl. Phys. Lett.* **105**, 181116 (2014).
- [14] R. Esteban, R. W. Taylor, J. J. Baumberg, and J. Aizpurua, *Langmuir* **28**, 8881 (2012).
- [15] H. Kitching, M. J. Shiers, A. J. Kenyon, and I. P. Parkin, *J. Mater. Chem. A* **1**, 6985 (2013).
- [16] D. Solis, B. Willingham, S. L. Nauert, L. S. Slaughter, J. Olson, P. Swanglap, A. Paul, W.-S. Chang, and S. Link, *Nano Lett.* **12**, 1349 (2012).
- [17] S. Chervinskii, V. Sevriuk, I. Reduto, and A. Lipovskii, *J. Appl. Phys.* **114**, 224301 (2013).
- [18] A. Klinkova, H. Thérien-Aubin, A. Ahmed, D. Nykypanchuk, R. M. Choueiri, B. Gagnon, A. Muntyanu, O. Gang, G. C. Walker, and E. Kumacheva, *Nano Lett.* **14**, 6314 (2014).
- [19] A. Alù and N. Engheta, *New J. Phys.* **12**, 013015 (2010).
- [20] V. A. Markel and A. K. Sarychev, *Phys. Rev. B* **75**, 085426 (2007).
- [21] F. Rütting, *Phys. Rev. B* **83**, 115447 (2011).
- [22] H. Cao, *Opt. Photon. News* **16**, 24 (2005).
- [23] D. S. Wiersma, *Nat. Phys.* **4**, 359 (2008).
- [24] D. S. Wiersma, *Nat. Photon.* **7**, 188 (2013).
- [25] M. Segev, Y. Silberberg, and D. N. Christodoulides, *Nat. Photon.* **7**, 197 (2013).
- [26] K. Vynck, M. Burreli, F. Riboli, and D. S. Wiersma, *Nat. Mater.* **11**, 1017 (2012).
- [27] I. M. Lifshits, S. A. Gredeskul, and L. A. Pastur, *Introduction to the Theory of Disordered Systems* (Wiley, New York, 1988), p. 462.
- [28] S. F. Liew and H. Cao, *J. Opt.* **12**, 024011 (2010).
- [29] A. N. Poddubny, M. V. Rybin, M. F. Limonov, and Y. S. Kivshar, *Nat. Commun.* **3**, 914 (2012).

- [30] A. Greshnov, M. Kaliteevski, R. Abram, S. Brand, and G. Zegrya, *Solid State Commun.* **146**, 157 (2008).
- [31] D. A. Genov, V. M. Shalaev, and A. K. Sarychev, *Phys. Rev. B* **72**, 113102 (2005).
- [32] M. I. Stockman, S. V. Faleev, and D. J. Bergman, *Phys. Rev. Lett.* **87**, 167401 (2001).
- [33] F. Dyson, *Phys. Rev.* **92**, 1331 (1953).
- [34] D. A. Parshin and H. R. Schober, *Phys. Rev. B* **57**, 10232 (1998).
- [35] Y. M. Beltukov and D. A. Parshin, *Phys. Solid State* **53**, 151 (2011).
- [36] H. Fidder and D. A. Wiersma, *J. Chem. Phys.* **95**, 7880 (1991).
- [37] G. G. Kozlov, V. A. Malyshev, F. Dominguez-Adame, and A. Rodriguez, *Phys. Rev. B* **58**, 5367 (1998).
- [38] I. Avgin and D. L. Huber, *Phys. Rev. B* **60**, 7646 (1999).
- [39] E. Wigner, *Ann. Math.* **62**, 548 (1955).
- [40] M. L. Mehta, *Random Matrices*, 3rd ed. (Elsevier, New York, 2004), p. 706.
- [41] E. Purcell, *Phys. Rev.* **69**, 674 (1946).
- [42] R. Sapienza, P. Bondareff, R. Pierrat, B. Habert, R. Carminati, and N. F. van Hulst, *Phys. Rev. Lett.* **106**, 163902 (2011).
- [43] L. Aigouy, A. Cazé, P. Gredin, M. Mortier, and R. Carminati, *Phys. Rev. Lett.* **113**, 076101 (2014).
- [44] L. Novotny and B. Hecht, *Principles of Nano-Optics* (Cambridge University, Cambridge, England, 2012), p. 578.
- [45] J.-W. Dong, K. H. Fung, C. T. Chan, and H.-Z. Wang, *Phys. Rev. B* **80**, 155118 (2009).
- [46] Z.-L. Deng, Z.-H. Li, J.-W. Dong, and H.-Z. Wang, *Plasmonics* **6**, 507 (2011).
- [47] V. A. Markel, *J. Phys.: Condens. Matter* **18**, 11149 (2006).
- [48] L. S. Slaughter, B. A. Willingham, W.-S. Chang, M. H. Chester, N. Ogden, and S. Link, *Nano Lett.* **12**, 3967 (2012).
- [49] G. Theodorou and M. H. Cohen, *Phys. Rev. B* **13**, 4597 (1976).
- [50] S. N. Evangelou, *J. Stat. Phys.* **69**, 361 (1992).
- [51] T. Rogers, I. P. Castillo, R. Kuhn, and K. Takeda, *Phys. Rev. E* **78**, 031116 (2008).
- [52] S. A. Maier, *Plasmonics: Fundamentals and Applications* (Springer, New York, 2007), p. 223.